Electronic Supplementary Material (ESI) for Soft Matter.

Supporting Material for "Cell-free layer development and spatial organization of healthy and rigid red blood cells in a microfluidic bifurcation"

Yazdan Rashidi[1], Othmane Aouane[2], Alexis Darras[1], Thomas John[1], Jens Harting[2,3], Christian Wagner[1,4], and Steffen M. Recktenwald[1,*]

[1]Dynamics of Fluids, Department of Experimental Physics, Saarland University, 66123 Saarbrücken, Germany
[2]Helmholtz Institute Erlangen-Nürnberg for Renewable Energy, Forschungszentrum Jülich, 91058 Erlangen, Germany
[3]Department of Chemical and Biological Engineering and Department of Physics, Friedrich-Alexander-Universität Erlangen-Nürnberg, 91058 Erlangen, Germany
[4]Department of Physics and Materials Science, University of Luxembourg, 1511 Luxembourg City, Luxembourg
[*]steffen.recktenwald@uni-saarland.de

Supplementary Figures

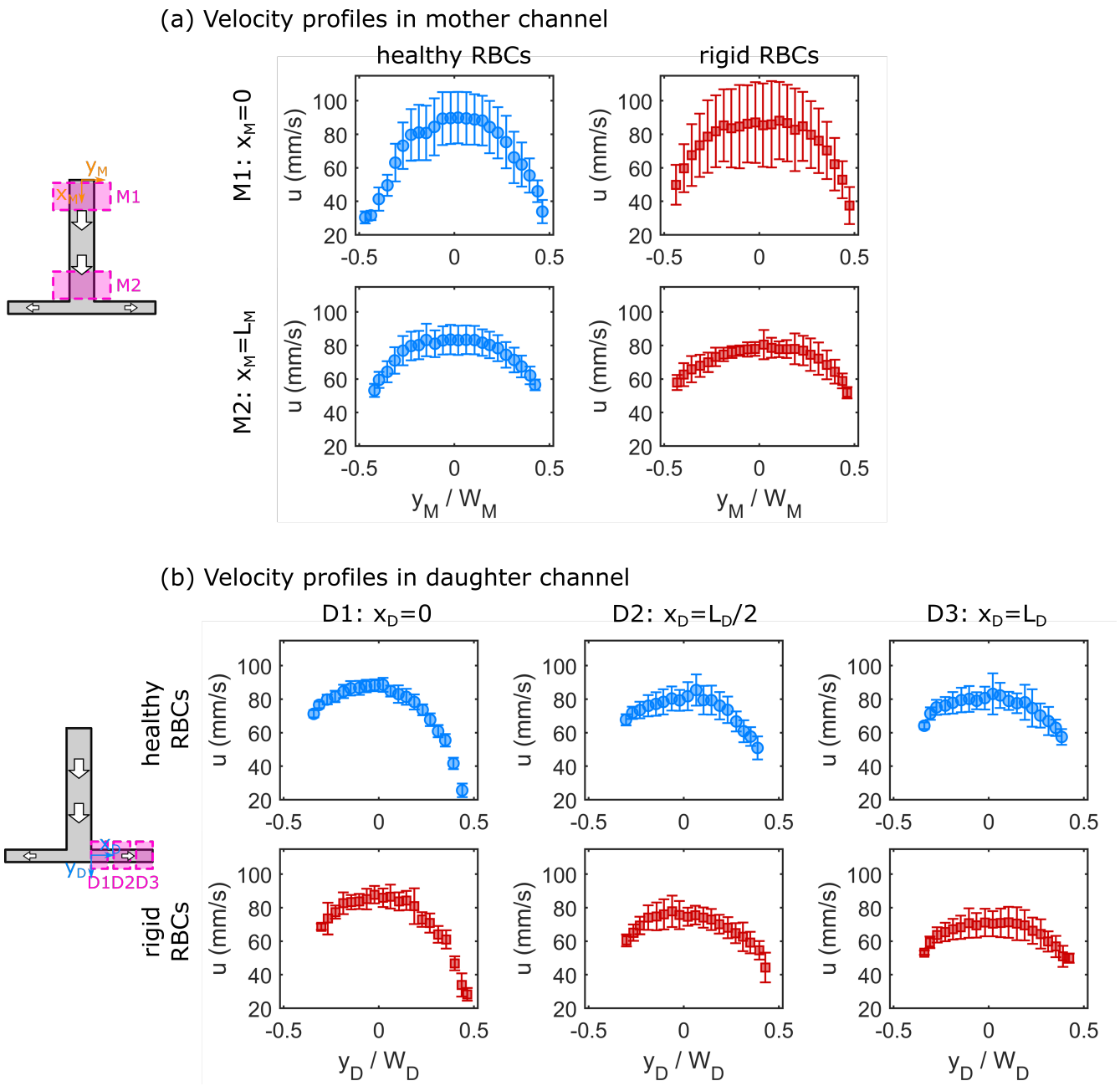

Figure S1 Velocity profiles at multiple positions in the T-junction. Data is representatively shown for a pressure drop of $p = 200\,\mathrm{mbar}$, which results in $\mathrm{Re} = 6$. (a) Velocity profiles in the mother channel for (left) healthy and (right) rigid RBCs at the (top) beginning ($x_\mathrm{M} \approx 0$) and (bottom) end ($x_\mathrm{M} = L_\mathrm{M}$) of the mother vessel. (b) Velocity profiles in the daughter channel for (top) healthy and (bottom) rigid cells at three positions along the flow direction.

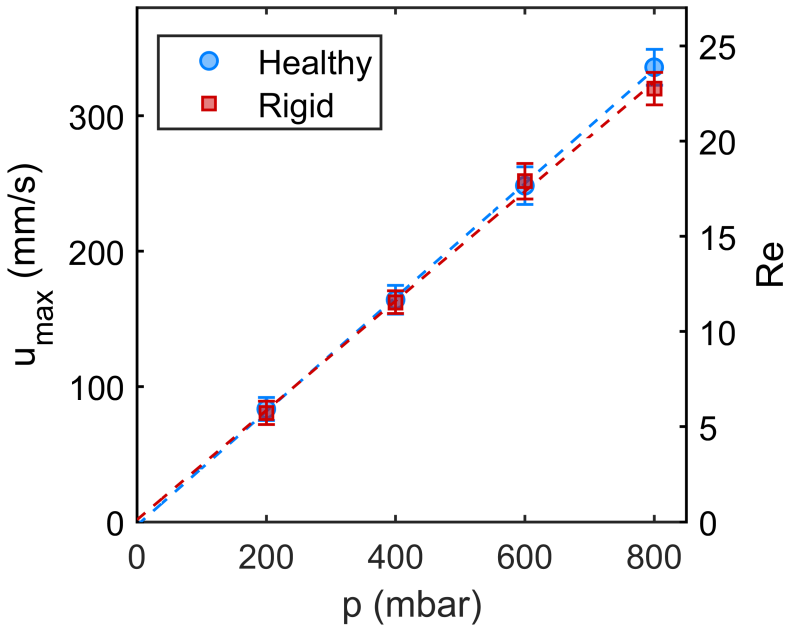

Figure S2 Maximum velocity $u_{\max}$ and Re as a function of the applied pressure drop p for healthy and rigid RBCs. Dashed lines correspond to linear fits of the experimental data.

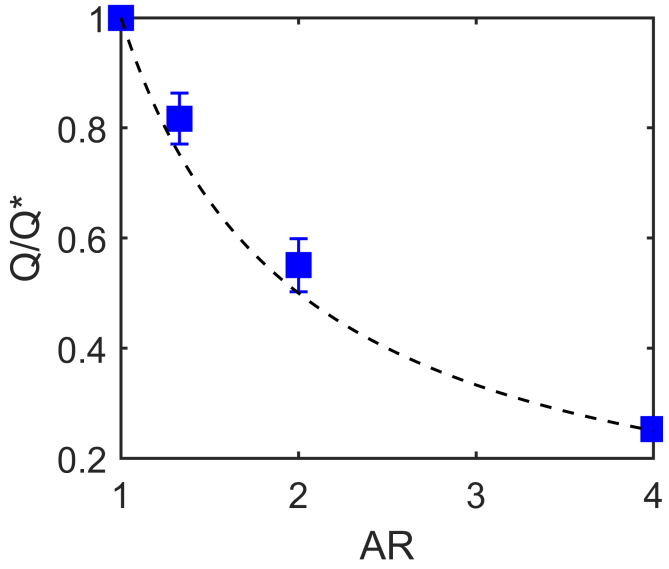

Figure S3 Ratio between the flow rates in the two daughter branches as a function of the asymmetry ratio at $p = 200\,\mathrm{mbar}$. Blue squares represent experimental data of the flow rate ratio based on the maximum velocities in both channels. The black dashed line corresponds to an analytical solution based on the length ratio $Q^*/Q \approx L_{\mathrm{D}}^*/L_{\mathrm{D}}$ between both channels. Error bars correspond to the standard deviation between different measurements.

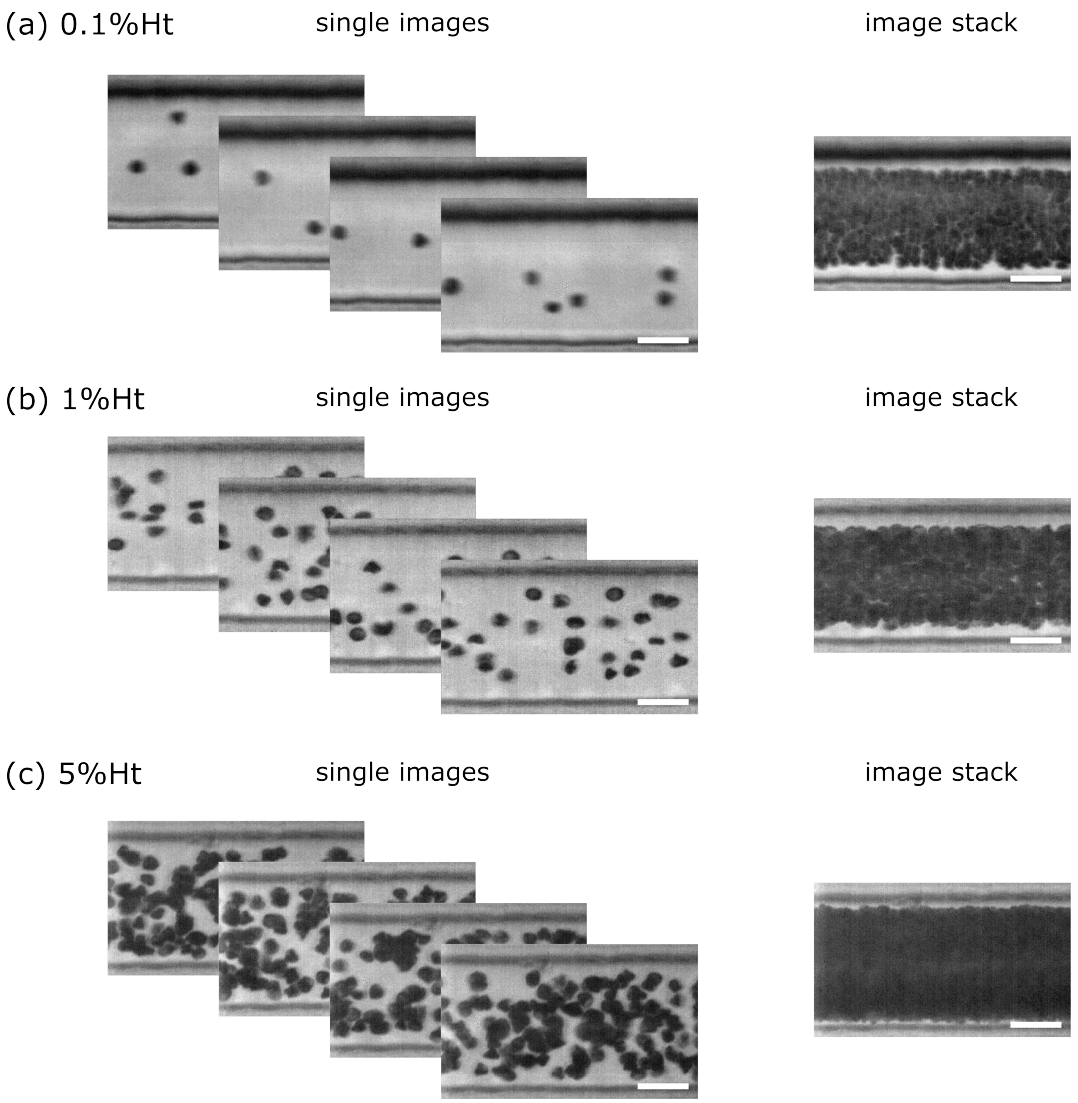

Figure S4 Representative single images and image stacks ($N = 250$) of the used RBC concentrations (a) $0.1\,\%\mathrm{Ht}$, (b) $1\,\%\mathrm{Ht}$, and (c) $5\,\%\mathrm{Ht}$. Scale bars represent $20\,\mu\mathrm{m}$.

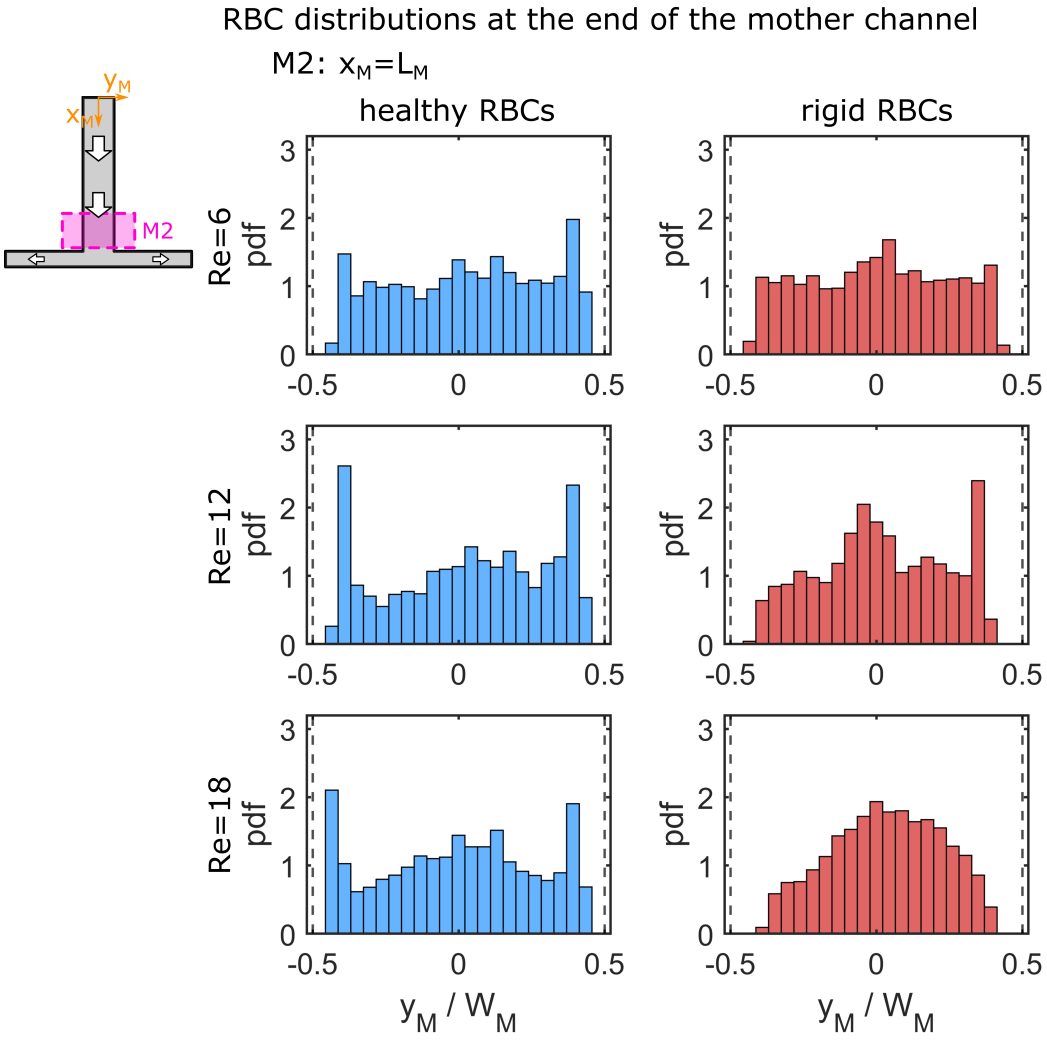

Figure S5 Effect of Re on the distributions for a healthy (left) and a rigid (right) $0.1\,\%\mathrm{Ht}$ RBC suspension in the mother channel. Distributions are shown at the end $x_\mathrm{M} = L_\mathrm{M}$ of the mother channel for different Re. Dashed vertical lines indicate the position of the channel borders at $y_\mathrm{M}/W_\mathrm{M} = \pm 0.5$.

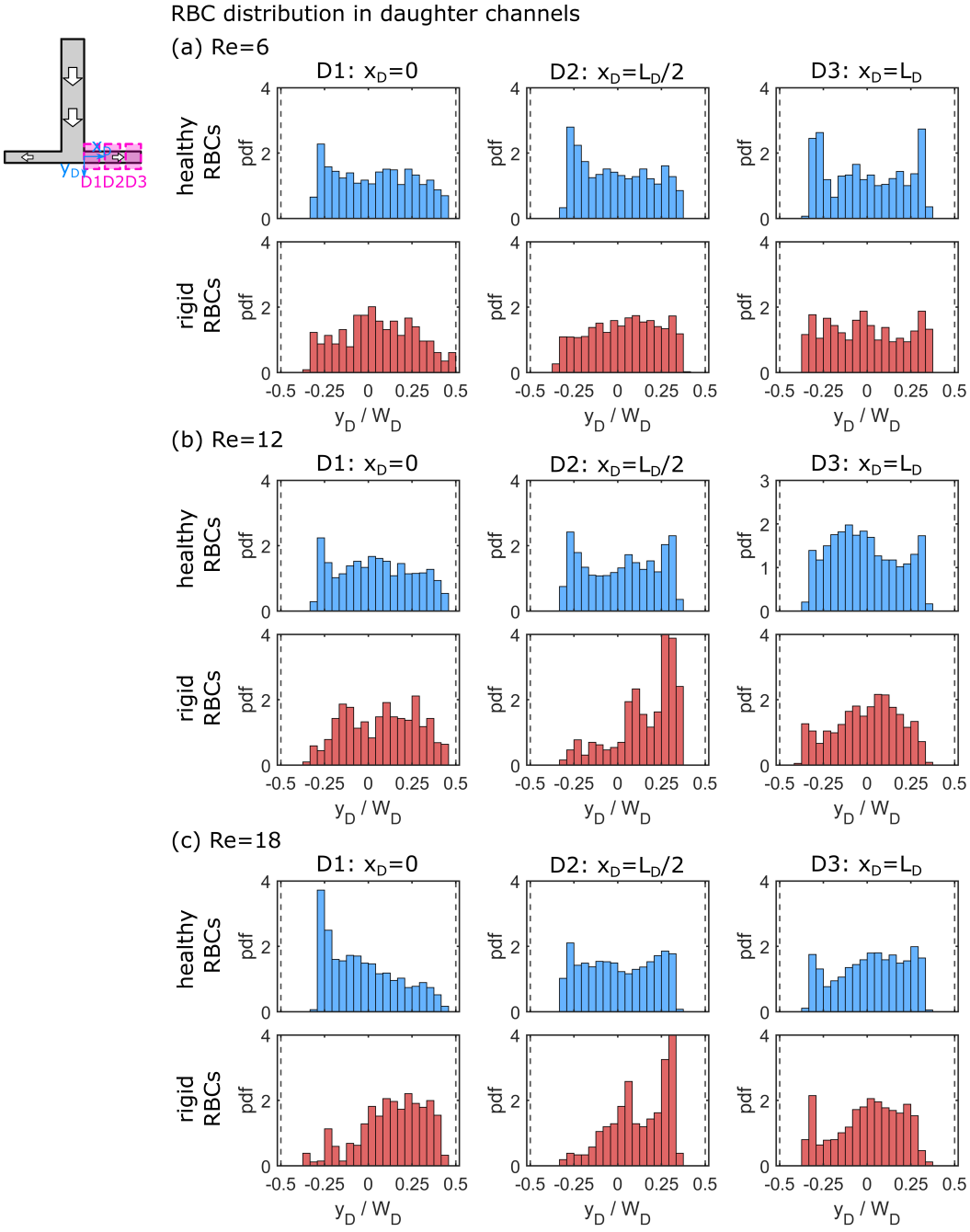

Figure S6 Effect of Re on the distribution of healthy and rigid RBCs at three positions along the flow direction in the daughter vessel. Dashed vertical lines indicate the position of the channel borders at $y_M/W_M = \pm 0.5$.

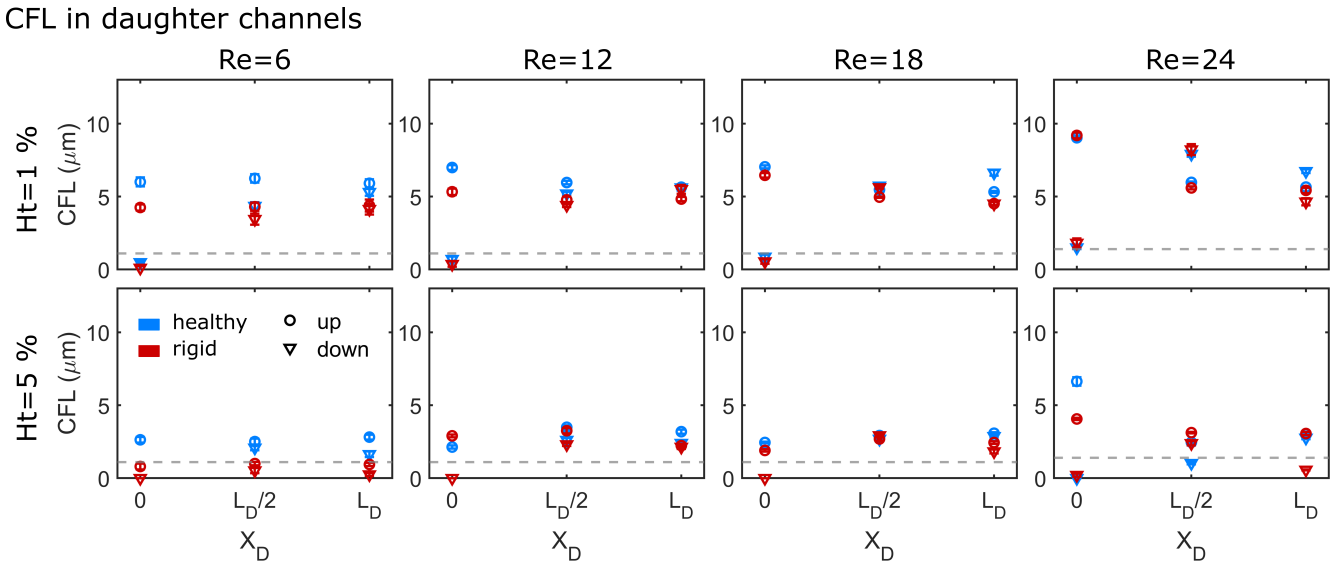

Figure S7 CFL development along the flow direction in the daughter vessels for different hematocrit and Re. CFL for a $1\,\%\mathrm{Ht}$ (top) and a $5\,\%\mathrm{Ht}$ (bottom) RBC suspensions at different Re and at three positions in the daughter channel.

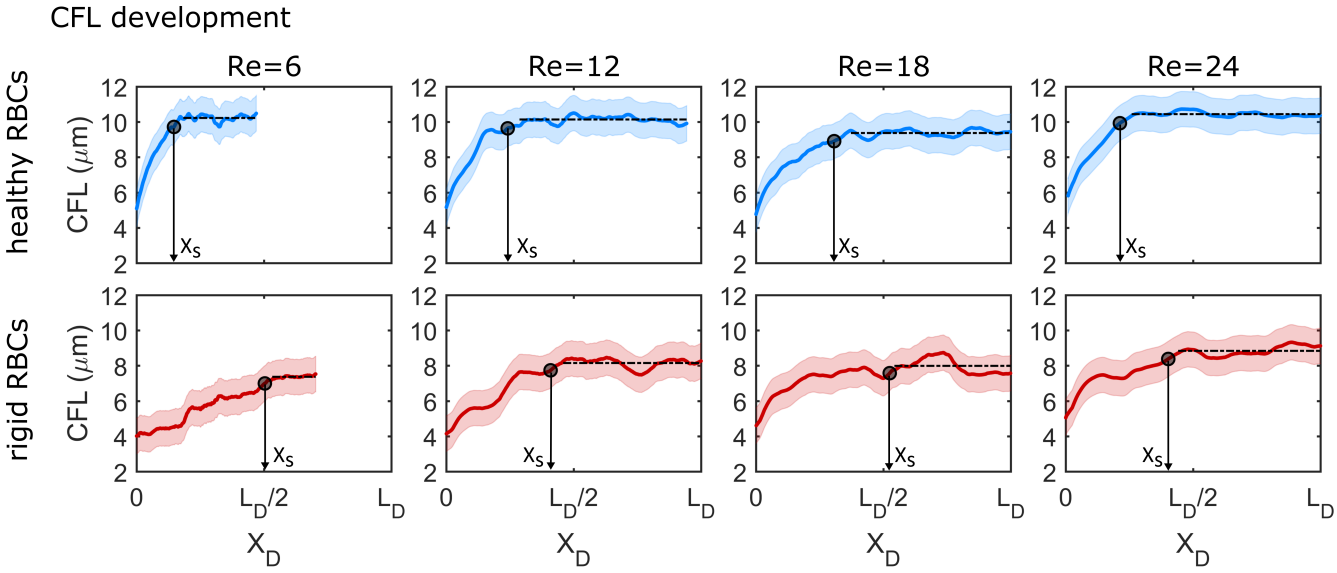

Figure S8 CFL development along the flow direction in the numerical simulations of healthy and rigid RBC suspension at $0.1\,\%\mathrm{Ht}$ in a straight channel at different Re. The x-axes are normalized by the length of the daughter branches L_D in the microfluidic experiments. The enveloping shaded areas correspond to $\pm 1\,\mu\mathrm{m}$, as discussed in the method section. Black, dashed horizontal lines indicate the mean steady-state CFL and the black circles represent the distance x_s that the RBCs travel until the steady-state CFL is reached.